Antiferromagnetic Dirac semimetals in two dimensions

Jing Wang
State Key Laboratory of Surface Physics and Department of Physics, Fudan University, Shanghai 200433, China and Collaborative Innovation Center of Advanced Microstructures, Nanjing 210093, China

(Received 11 September 2016; revised manuscript received 2 March 2017; published 21 March 2017)

The search for symmetry-protected two-dimensional (2D) Dirac semimetals analogous to graphene is important both for fundamental and practical interest. The 2D Dirac cones are protected by crystalline symmetries and magnetic ordering may destroy their robustness. Here we propose a general framework to classify stable 2D Dirac semimetals in spin-orbit coupled systems having the combined time-reversal and inversion symmetries, and show the existence of the stable Dirac points in 2D antiferromagnetic semimetals. Compared to 3D Dirac semimetals which fall into two distinct classes, Dirac semimetals in 2D with combined time-reversal and inversion symmetries belong to a single class which is closely related to the nonsymmorphic space-group symmetries. We further provide a concrete model in antiferromagnetic semimetals which supports symmetry-protected 2D Dirac points. The symmetry breaking in such systems leads to 2D chiral topological states such as quantum anomalous Hall insulator and chiral topological superconductor phases.

DOI: 10.1103/PhysRevB.95.115138

I. INTRODUCTION

The discovery of the time-reversal invariant topological insulators [1,2] greatly inspired the study of symmetry-protected Dirac semimetals (DSMs) [3–14]. In a DSM, the low-energy physics is well described by pseudorelativistic Dirac fermions with linear energy dispersions along all momentum directions around Dirac points (DPs) in the Brillouin zone (BZ). To guarantee the robustness of three-dimensional (3D) DPs, the crystalline symmetry protection is a necessity [7], similar to the 2D DPs in graphene [15]. The 3D DSM materials [3–11] have both the time-reversal symmetry $\mathcal{T}$ and inversion symmetry $\mathcal{P}$. The $\mathcal{T}$ or $\mathcal{P}$ breaking, in general, leads to Weyl semimetals [16–27], where the DPs split into Weyl points. However, under certain conditions, such 3D DPs still remain stable with $\mathcal{T}$ broken [28]. This motivates us to ask whether stable DPs could exist in 2D in the absence of $\mathcal{T}$ and $\mathcal{P}$. The positive answer to this question will lead to many interesting physical phenomena and novel topological states, as expected from the great success in the field of graphene.

Recently, the concept of 2D DSMs in the presence of spin-orbit coupling (SOC) has been introduced by Young and Kane [29], where the nonsymmorphic space-group symmetries play a key role [29–33]. In this paper, we study the 2D Dirac fermions in antiferromagnetic (AFM) semimetals. A general framework is proposed to classify stable 2D DSMs in SOC systems with $\mathcal{PT}$ symmetry. In sharp contrast to $\mathcal{T}$-invariant 3D DSMs which fall into two distinct classes [7], DSMs in 2D with $\mathcal{PT}$ symmetry only have one class. The DPs of 2D DSMs reside at the BZ boundary which are protected by the nonsymmorphic space-group symmetries. We further provide a tight-binding model in AFM semimetals which supports symmetry-protected 2D DPs and symmetry breaking in such systems leads to exotic chiral topological states in 2D. We conclude with a brief discussion on the possible material venues for such phases.

The 2D DP with fourfold degeneracy is generated when two doubly degenerate energy bands avoidably cross. The most common symmetry for crystalline solids to have double degeneracy of bands is $\mathcal{PT}$ symmetry satisfying $(\mathcal{PT})^2=-1$, which includes two cases with both $\mathcal{T},\mathcal{P}$ conserved and $\mathcal{T},\mathcal{P}$ broken. Under this condition, the low-energy physics can be described by the minimal four-band effective Hamiltonian,

$$\mathcal{H}(\mathbf{k}) = \epsilon_0(\mathbf{k}) + \sum_{a=1}^{5} d_a(\mathbf{k})\Gamma_a, \tag{1}$$

where Γ_a are 4×4 Dirac Γ matrices satisfying $\{\Gamma_a,\Gamma_b\}=2\delta_{ab}$, and the specific representation of Γ_a depends on the crystalline symmetry. The particle-hole asymmetry term $\epsilon_0(\mathbf{k})$ is neglected for simplicity, $d_a(\mathbf{k})$ $(a=1,\ldots,5)$ are real functions of $\mathbf{k}$, and $\mathbf{k}=(k_x,k_y)$. The energy spectrum is

$$E_{\pm}(\mathbf{k}) = \pm\sqrt{\sum_{a=1}^{5} d_a^2(\mathbf{k})}. \tag{2}$$

The DPs can be generated only when all $d_a(\mathbf{k})=0$ for certain $\mathbf{k}$ in the BZ. A simple case for this condition exists at the quantum critical point of the phase transition between a quantum spin Hall (QSH) and a normal insulator (NI) in the presence of $\mathcal{T}$ and $\mathcal{P}$ [16,34]. Such DPs are accidental degeneracies and not robust against perturbations. Therefore, crystalline symmetry is needed to protect the 2D DPs.

The organization of this paper is as follows. Section II describes the general framework to classify stable 2D DSM with $\mathcal{PT}$ symmetry. Section III presents a magnetic tight-binding model which supports symmetry-protected 2D DPs, and the symmetry-breaking phases. Section IV presents a discussion of the possible material venues for 2D AFM DSMs and concludes this paper. Some auxiliary materials are relegated to the appendices.

II. GENERAL THEORY

The basic mechanism for the avoidable crossing of energy bands is to let the bands have different symmetry representations [7,29,35]. We start with classifying stable DSMs of 2D SOC systems in the presence of $\mathcal{PT}$ and crystalline symmetry such as rotational and mirror symmetries. The generic Hamiltonian has the form $\mathcal{H}(\mathbf{k})=\sum_{i,j=0}^{3} d_{ij}(\mathbf{k})\sigma_i\otimes$

τ_j, where σ_i and τ_i ($i = 1,2,3$) are Pauli matrices acting on the spin and orbital, respectively. σ_0 and τ_0 are 2×2 identity matrices. $d_{ij}(\mathbf{k})$ are real functions of $\mathbf{k}$. The invariance of the system will set many terms to be zero or nonindependent, which reduces to the effective Hamiltonian in Eq. (1).

A. Case A: $\mathcal{T}$, $\mathcal{P}$ conserved

The $\mathcal{T}$ operator is $\mathcal{T} = i\sigma_2\mathcal{K}$, where $\mathcal{K}$ is the complex conjugation; $\mathcal{H}(-\mathbf{k}) = \mathcal{T}\mathcal{H}(\mathbf{k})\mathcal{T}^{-1}$. $\mathcal{P}$ is independent of the spin rotation, where its specific form is determined by $\mathcal{P}^\dagger\mathcal{P} = 1$, $[\mathcal{T},\mathcal{P}] = 0$, and $(\mathcal{P}\mathcal{T})^2 = -1$. Thus, $\mathcal{P} = \pm\tau_0$, $\pm\tau_3$, or $\pm\tau_1$; $\mathcal{H}(-\mathbf{k}) = \mathcal{P}\mathcal{H}(\mathbf{k})\mathcal{P}^{-1}$. If $\mathcal{P} = \pm\tau_1$, $\Gamma^{(1,2,3,4,5)} = (\sigma_3 \otimes \tau_3, \tau_2, \sigma_1 \otimes \tau_3, \sigma_2 \otimes \tau_3, \tau_1)$, and $d_a(\mathbf{k}) = -d_a(-\mathbf{k})$ for $a = 1,\ldots,4$, $d_5(\mathbf{k}) = d_5(-\mathbf{k})$. All $d_a(\mathbf{k}) = 0$ satisfied simultaneously leads to DPs; however, the number of equations is larger than the number of variables k_x, k_y and the external parameter m. Therefore, the band crossing will not happen at generic $\mathbf{k}$. The crystalline symmetry will further set constraints on $d_a(\mathbf{k})$. In 2D, the relevant symmetries are $C_{2\hat{x}}$, $C_{2\hat{y}}$, $M_{\hat{z}}$, and $C_{n\hat{z}}$.

$C_{2\hat{x}}$ *symmetry.* The invariance of the system under π rotation along the x axis requires $C_{2\hat{x}}\mathcal{H}(k_x,k_y)C_{2\hat{x}}^{-1} = \mathcal{H}(k_x,-k_y)$. $k_y = 0$ along the k_x axis, $[C_{2\hat{x}},\mathcal{H}(k_x,0)] = 0$. Therefore, we can choose a basis to make both $C_{2\hat{x}}$ and $\mathcal{H}(k_x)$ diagonal. In such a basis, the explicit forms of $C_{2\hat{x}}$ are obtained by the constraint $[\mathcal{T},C_{2\hat{x}}] = 0$. Therefore, $C_{2\hat{x}} = \mathrm{diag}[\alpha_p,\alpha_q,\alpha_p^*,\alpha_q^*]$, where $\alpha_p = \exp[i\pi(p + \frac{1}{2})]$ with $p = 0,1$. Thus we have $C_{2\hat{x}} = i\sigma_3$, or $i\sigma_3 \otimes \tau_3$. With the explicit representations of $C_{2\hat{x}}$ and $\mathcal{P}$ operators, we can get the symmetry-allowed forms of $d_a(\mathbf{k})$. Take $\mathcal{P} = \pm\tau_1$ for example; when $C_{2\hat{x}} = i\sigma_3 \otimes \tau_3$, to the leading order in $\mathbf{k}$, the symmetry constraints lead to $d_{1,2,3,4,5}(\mathbf{k}) = (v_1k_x, v_2k_y, v_3k_y, v_4k_y, v_5k_xk_y)$, where v_i are coefficients. This is simply the 2D DSM with anisotropic linear dispersions. Considering the full periodic structure of the BZ, the time-reversal invariant momentum (TRIM) $(\pi,0)$, $(0,\pi)$ and (π,π) are possible locations of the 2D DPs. The (0,0) point is simply excluded because the symmetry-protected DPs are not compatible with threefold rotation, while the space groups admit the 4D representations at (0,0) contain $C_{3\hat{z}}$ [3,36]. Similarly, when $C_{2\hat{x}} = i\sigma_3$, $d_{1,2,3,4,5}(\mathbf{k}) = (v_1k_x, v_2k_x, v_3k_y, v_4k_y, m + u_1k_x^2 + u_2k_y^2)$, where v_i, u_i, and m are constants. This is not a DSM Hamiltonian. However, it is worthwhile to mention that critical DPs indeed exist at TRIM at the transition between QSH and NI [16] as shown in Fig. 4(b). At the TRIM point, $\mathbf{k}$ and $-\mathbf{k}$ are equivalent and all odd functions in $\mathcal{H}(\mathbf{k})$ vanish. By tuning m, $d_5(\mathbf{k},m) = 0$ is satisfied.

The classification of 2D DSMs for case A is shown in Table I. The details of 2D DPs protected by $M_{\hat{z}}$ and $C_{n\hat{z}}$ are discussed in Appendix A. The stable DPs exist at the TRIM of the BZ boundary and are protected by the lattice symmetry, including symmorphic and nonsymmorphic symmetries [29]. In nonsymmorphic symmetric systems with two sublattices, $\mathcal{P} = \pm\tau_1$ is the inversion operator with sublattices interchanged [7], which is realized by the inversion with respect to a lattice site followed by a fraction translation.

TABLE I. The classification table of 2D DSMs for case A with both $\mathcal{T}$ and $\mathcal{P}$ symmetries; $\ell = 2,4,6$. The DPs are induced by the topological band crossing at the BZ boundary.

Symmetry	$\mathcal{P}$	$\mathcal{T}$	Dispersion
$C_{2\hat{x}} = i\sigma_3 \otimes \tau_3$	$\pm\tau_1$	$i\sigma_2\mathcal{K}$	Linear
$M_{\hat{z}} = \sigma_3 \otimes \tau_2$	$\pm\tau_1$	$i\sigma_2\mathcal{K}$	Linear
$C_{\ell\hat{z}} = e^{i\frac{\pi}{\ell}\sigma_3} \otimes \tau_3$	$\pm\tau_1$	$i\sigma_2\mathcal{K}$	Linear
$C_{6\hat{z}} = e^{i\frac{\pi}{2}\sigma_3} \otimes \tau_3$	$\pm\tau_1$	$i\sigma_2\mathcal{K}$	Cubic

B. Case B: $\mathcal{T}$, $\mathcal{P}$ broken

The antiunitary $\mathcal{P}\mathcal{T}$ symmetry reverses spins and keeps $\mathbf{k}$ invariant. Without loss of generality, in this section we set $\mathcal{P}\mathcal{T} = i\sigma_2\mathcal{K}$. With $[\mathcal{P}\mathcal{T},\mathcal{H}(\mathbf{k})] = 0$, one has $\mathcal{H}(\mathbf{k}) = d_1\tau_1 + d_2\sigma_3 \otimes \tau_2 + d_3\sigma_1 \otimes \tau_2 + d_4\sigma_2 \otimes \tau_2 + d_5\tau_3$. The crystalline symmetries fall into two classes: symmorphic and nonsymmorphic space-group symmetries, the operations of which are denoted as $\{g|\mathbf{t}\}$ and can be constructed by the point group operations g with translation $\mathbf{t}$ that are a full and a fraction of a Bravais lattice vector, respectively. In 2D, the representative symmorphic-group symmetries are $\{C_{2\hat{x}}|00\}$, $\{C_{2\hat{y}}|00\}$, $\{M_{\hat{z}}|00\}$, and $C_{n\hat{z}}$. The typical 2D nonsymmorphic-group operations include screw rotation $\{C_{2\hat{x}}|\mathbf{t}\}$, $\{C_{2\hat{y}}|\mathbf{t}\}$, glide mirror lines $\{M_{\hat{x}}|\mathbf{t}\}$, $\{M_{\hat{y}}|\mathbf{t}\}$, and glide mirror plane $\{M_{\hat{z}}|\mathbf{t}\}$, where $\mathbf{t}$ is a half translation which satisfies $g\mathbf{t} = \mathbf{t}$ and $e^{i\mathbf{G}\cdot\mathbf{t}} = -1$ for odd reciprocal lattice vector $\mathbf{G}$. Explicitly, in units of Bravais lattice constant, $\mathbf{t} = (\frac{1}{2},0),(0,\frac{1}{2}),(\frac{1}{2},\frac{1}{2})$. In the following, we will show that stable 2D DPs can only exist in the presence of nonsymmorphic symmetries:

(i) For the *symmorphic group*, we take $\{M_{\hat{z}}|00\}$ for example; $\mathbf{k}$ is invariant and $(\sigma_1,\sigma_2,\sigma_3) \to (-\sigma_1,-\sigma_2,\sigma_3)$. The symmetry constraints on $d_a(\mathbf{k})$ are $d_{3,4}(\mathbf{k}) = 0$. To the lowest order in $\mathbf{k}$, the general form is $d_a(\mathbf{k}) = m_a + v_a^xk_x + v_a^yk_y$ for $a = 1,2,5$, and m_a, v_a^x, v_a^y are coefficients. The DPs are not guaranteed and can only be generated by fine tuning. Even with the extra $\{C_{2\hat{x}}|00\}$ or $\{C_{2\hat{y}}|00\}$ symmetry, it only constrains $d_2(\mathbf{k}) = v_2^yk_y$, and still the DPs are not guaranteed.

(ii) For the *nonsymmorphic group*, we take $\{C_{2\hat{x}}|\frac{1}{2}\frac{1}{2}\}$ for example. Under $\{C_{2\hat{x}}|\frac{1}{2}\frac{1}{2}\}$, $(x,y) \to (x + \frac{1}{2}, -y + \frac{1}{2})$, $(k_x,k_y) \to (k_x,-k_y)$, and $(\sigma_1,\sigma_2,\sigma_3) \to (\sigma_1,-\sigma_2,-\sigma_3)$; $\{C_{2\hat{x}}|\frac{1}{2}\frac{1}{2}\}\mathcal{H}(k_x,k_y)\{C_{2\hat{x}}|\frac{1}{2}\frac{1}{2}\}^{-1} = \mathcal{H}(k_x,-k_y)$. Thus, $\{C_{2\hat{x}}|\frac{1}{2}\frac{1}{2}\}^2 = -e^{-ik_x}$ is just a full translation along the x axis with a 2π rotation of spins. $\mathcal{H}(\mathbf{k})$ is invariant under $\{C_{2\hat{x}}|\frac{1}{2}\frac{1}{2}\}$ along $k_y = 0,\pi$ lines. Therefore, both $\{C_{2\hat{x}}|\frac{1}{2}\frac{1}{2}\}$ and $\mathcal{H}(k_x)$ can be chosen as diagonal. The exact representation of the $\{C_{2\hat{x}}|\frac{1}{2}\frac{1}{2}\}$ operator is obtained by noticing

$$\left\{C_{2\hat{x}}|\frac{1}{2}\frac{1}{2}\right\}\mathcal{P}\mathcal{T} = e^{-ik_x}e^{-ik_y}\mathcal{P}\mathcal{T}\left\{C_{2\hat{x}}|\frac{1}{2}\frac{1}{2}\right\}. \qquad (3)$$

Thus, $\{C_{2\hat{x}}|\frac{1}{2}\frac{1}{2}\} = ie^{-ik_x/2}\sigma_3$, or $ie^{-ik_x/2}\sigma_3 \otimes \tau_3$ when $k_y = 0$; and $\{C_{2\hat{x}}|\frac{1}{2}\frac{1}{2}\} = ie^{-ik_x/2}\tau_3$ when $k_y = \pi$. However, there is only one case in which the stable band crossing and Dirac Hamiltonian can appear, namely, $\{C_{2\hat{x}}|\frac{1}{2}\frac{1}{2}\} = ie^{-ik_x/2}\tau_3$ along the $k_y = \pi$ line, where only the $d_5(k_x,\pi)$ term is present. If $d_5(k_x,\pi) = 0$ at $\mathbf{k}_0 = (k_{x0},\pi)$, then around the $\mathbf{k}_0$ point, to the leading order, the effective Hamiltonian is Dirac like and expanded as $d_{1,2,3,4,5}(\mathbf{k}) = (v_1k_y, v_2k_y, v_3k_y, v_4k_y, v_5k_x)$, where v_i are real. There is an alternative way to see why topological band crossing can only exist along the $k_y = \pi$ line. The two Bloch states $|u_\mathbf{k}^+\rangle$, $|u_\mathbf{k}^-\rangle$ and their $\mathcal{P}\mathcal{T}$ partners $\mathcal{P}\mathcal{T}|u_\mathbf{k}^+\rangle$,

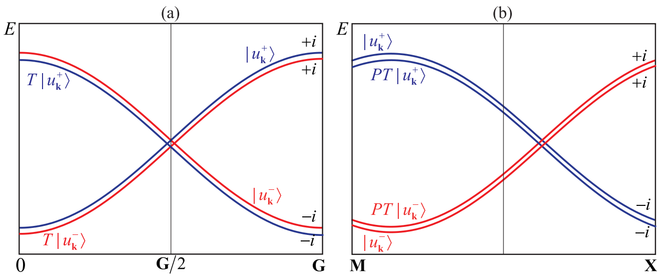

FIG. 1. A nonsymmorphic symmetry $\{g|\mathbf{t}\}$ ensures band crossing on a g invariant line at the BZ boundary. The doubly degenerate bands are artificially split for clarity. (a) With $\mathcal{P}$ and $\mathcal{T}$, and $\mathcal{P}=\tau_1$, Bloch states $(|u_{\mathbf{k}}^{+}\rangle,\mathcal{T}|u_{\mathbf{k}}^{-}\rangle)$ and $(|u_{\mathbf{k}}^{-}\rangle,\mathcal{T}|u_{\mathbf{k}}^{+}\rangle)$ carry different representations of $\{g|\mathbf{t}\}$ ($C_{2\hat{x}}$, for example) and cross at TRIM. (b) Without $\mathcal{P}$ and $\mathcal{T}$, but with combined $\mathcal{PT}$, $(|u_{\mathbf{k}}^{+}\rangle,\mathcal{PT}|u_{\mathbf{k}}^{+}\rangle)$ and $(|u_{\mathbf{k}}^{-}\rangle,\mathcal{PT}|u_{\mathbf{k}}^{-}\rangle)$ have different eigenvalues of $\{C_{2\hat{x}}|\frac{1}{2}\frac{1}{2}\}$ and cross avoidably.

$\mathcal{PT}|u_{\mathbf{k}}^{-}\rangle$ are eigenstates of $\{C_{2\hat{x}}|\frac{1}{2}\frac{1}{2}\}$, which is $\pm ie^{-ik_x/2}$. $|u_{\mathbf{k}}^{\pm}\rangle$ has the same energy as its $\mathcal{PT}$ partner. To have a stable band crossing, $(|u_{\mathbf{k}}^{+}\rangle,\mathcal{PT}|u_{\mathbf{k}}^{+}\rangle)$ and $(|u_{\mathbf{k}}^{-}\rangle,\mathcal{PT}|u_{\mathbf{k}}^{-}\rangle)$ should carry different representations of $\{C_{2\hat{x}}|\frac{1}{2}\frac{1}{2}\}$, as shown in Fig. 1(b). This is only possible as $\{C_{2\hat{x}}|\frac{1}{2}\frac{1}{2}\}=ie^{-ik_x/2}\tau_3$ along $k_y=\pi$.

As shown in Table II, the stable DPs can indeed exist in certain AFM semimetals respecting $\mathcal{PT}$ symmetry. The DPs in both $\mathcal{T}$-invariant and $\mathcal{T}$-broken semimetals are generated by the avoidable crossing of energy bands with distinct representations, which are protected by nonsymmorphic symmetries. However, different from the $\mathcal{T}$-invariant semimetals where the DPs reside at TRIMs of the BZ boundary, here the DPs in $\mathcal{T}$-broken systems can only appear at the BZ boundary but not at TRIMs in general. Moreover, the glide mirror plane symmetry $M_{\hat{z}}$ cannot protect the DPs with $\mathcal{T}$ broken, as listed in Appendix B, contrary to its protection of DPs with $\mathcal{T}$. More importantly, the DPs in the $\mathcal{T}$-broken AFM DSMs are locally permitted by crystalline symmetries, while the DPs in $\mathcal{T}$-invariant DSMs are essential and cannot be gapped without lowering the specific space-group symmetries.

III. MODEL

A. Tight-binding model

Now we study a tight-binding model for a 2D AFM DSM to illustrate the nonsymmorphic symmetry-protected DPs listed in Table II. For direct comparison with the $\mathcal{T}$-invariant case, we adopted the lattice similar to Ref. [29]; as shown in Fig. 2(a), the system has a layered AFM structure with two atoms in one unit cell, denoted as A and B. The lattice vectors are denoted as $\vec{\mathbf{a}}_1=(1,0,0)$, $\vec{\mathbf{a}}_2=(0,1,0)$. In each unit cell, the A and B atoms are shifted along the z axis with the position $r_A=(-\frac{1}{4},-\frac{1}{4},-\frac{c}{2})$ and $r_B=(\frac{1}{4},\frac{1}{4},\frac{c}{2})$. Without AFM ordering, this structure is in space-group no. 129 ($P4/nmm$). Each lattice site contains a d_{z^2} orbital, where the square pyramidal crystal field splits d_{z^2} from other d orbitals. The Hamiltonian is

$$\mathcal{H}=t\sum_{\langle ij\rangle}c_i^{\dagger}c_j+\sum_{\langle\langle ij\rangle\rangle}c_i^{\dagger}[t_2+i\lambda_{\rm so}(\hat{\mathbf{d}}_1\times\hat{\mathbf{d}}_2)\cdot\mathbf{s}]c_j +\Delta\sum_i\xi_i c_i^{\dagger}\mathbf{s}\cdot\hat{\mathbf{n}}c_i, \tag{4}$$

where $\langle ij\rangle$ and $\langle\langle ij\rangle\rangle$ denote the nearest- and next-nearest-neighbor sites, respectively. $\lambda_{\rm so}$ is a SOC which involves spin-dependent next-nearest-neighbor hopping, where $\hat{\mathbf{d}}_1$ and $\hat{\mathbf{d}}_2$ are unit vectors along two nearest-neighbor bonds hopping from site j to i [37]. $\mathbf{s}$ describes the electron spins. The third term is the staggered Zeeman term ($\xi_i=\pm1$), which describes the AFM ordering (along the $\hat{\mathbf{n}}$ direction).

The symmetry of the system depends on the AFM order direction. In Fig. 2(a), if $\hat{\mathbf{n}}=\hat{z}$, the system breaks $\mathcal{T}$ and $\mathcal{P}$ but respects $\mathcal{PT}$. However, from the energy bands, the screw axes $\{C_{2\hat{x}}|\frac{1}{2}0\}$ and $\{C_{2\hat{y}}|0\frac{1}{2}\}$ cannot protect the DPs, consistent with the analysis in Table II. This is quite different from the $\mathcal{T}$-, $\mathcal{P}$-invariant case (dashed line), where the DPs at X_1, M, and X_2 are protected by $\{C_{2\hat{x}}|\frac{1}{2}0\}$ and $\{C_{2\hat{y}}|0\frac{1}{2}\}$ [29]. In Fig. 2(b), if $\hat{\mathbf{n}}=\hat{x}$, two DPs are located along the X_1-M line, and they are at different energies in the presence of the t_2 term. The Hamiltonian

$$\mathcal{H}(\mathbf{k})=4t\tau_1\cos\frac{k_x}{2}\cos\frac{k_y}{2}+2t_2(\cos k_x+\cos k_y) +2\lambda_{\rm so}\sigma_2\otimes\tau_3\sin k_x+(\Delta-2\lambda_{\rm so}\sin k_y)\sigma_1\otimes\tau_3.$$

The DPs are at $\mathbf{k}_1=(\pi,k_{y0})$ and $\mathbf{k}_2=(\pi,\pi-k_{y0})$, where $\sin k_{y0}=\Delta/2\lambda_{\rm so}$. These two inequivalent DPs are protected by $\{M_{\hat{x}}|\frac{1}{2}0\}$. This can be seen by examining the effective model near these points. Near $\mathbf{k}=\mathbf{k}_1$,

$$\mathcal{H}(\mathbf{k}_1+\mathbf{q})=-2t\cos\frac{k_{y0}}{2}\tau_1q_x-2\lambda_{\rm so}\sigma_2\otimes\tau_3q_x -2\lambda_{\rm so}\cos k_{y0}\sigma_1\otimes\tau_3q_y. \tag{5}$$

At $\mathbf{k}_1$, the symmetry $\mathcal{PT}=i\sigma_2\mathcal{K}\otimes\tau_1$ allows the mass terms τ_2 and $\sigma_3\otimes\tau_3$. This is forbidden by $\{M_{\hat{x}}|\frac{1}{2}0\}=i\sigma_1\otimes\tau_3$, but is allowed by $\{C_{2\hat{y}}|0\frac{1}{2}\}=\sigma_2\otimes\tau_2$. There is a subtle point, it seems $\{M_{\hat{z}}|\frac{1}{2}\frac{1}{2}\}=\sigma_3\otimes\tau_1$ could also forbid the mass terms. To further clarify the role of $\{M_{\hat{x}}|\frac{1}{2}0\}$ and $\{M_{\hat{z}}|\frac{1}{2}\frac{1}{2}\}$ in protecting the DPs, we distorted the lattice which eliminates $\{M_{\hat{x}}|\frac{1}{2}0\}$ and keeps $\{M_{\hat{z}}|\frac{1}{2}\frac{1}{2}\}$ in Fig. 2(c). Such distortion adds a term to nearest-neighbor hopping $\mathcal{H}_1=t_3\sin(k_x/2)\sin(k_y/2)\tau_1$, which will gap the DPs at $\mathbf{k}_{1,2}$, consistent with DPs not being protected by $\{M_{\hat{z}}|\frac{1}{2}\frac{1}{2}\}$. In Fig. 2(d), the B site is shifted along the y axis, which breaks $\{M_{\hat{z}}|\frac{1}{2}\frac{1}{2}\}$ but keeps $\{M_{\hat{x}}|\frac{1}{2}0\}$. Such reduced symmetry allows a term $\mathcal{H}_2=\cos(k_x/2)\sin(k_y/2)(t_4\tau_1+t_5\tau_2)$, where the DPs located along the X_1-M line remain protected. However, it is noted that these two inequivalent DPs always appear or disappear together.

TABLE II. The classification table of 2D DSMs for case B with $\mathcal{T}$ and $\mathcal{P}$ broken. The nonsymmorphic symmetries with the corresponding half translation $\mathbf{t}$ are indicated.

Symmetry	Half translation $\mathbf{t}$	Dispersion
$\{C_{2\hat{x}}|\mathbf{t}\}$	$\mathbf{t}=(0,\frac{1}{2}),(\frac{1}{2},\frac{1}{2})$	Linear
$\{C_{2\hat{y}}|\mathbf{t}\}$	$\mathbf{t}=(\frac{1}{2},0),(\frac{1}{2},\frac{1}{2})$	Linear
$\{M_{\hat{x}}|\mathbf{t}\}$	$\mathbf{t}=(\frac{1}{2},0),(\frac{1}{2},\frac{1}{2})$	Linear
$\{M_{\hat{y}}|\mathbf{t}\}$	$\mathbf{t}=(0,\frac{1}{2}),(\frac{1}{2},\frac{1}{2})$	Linear

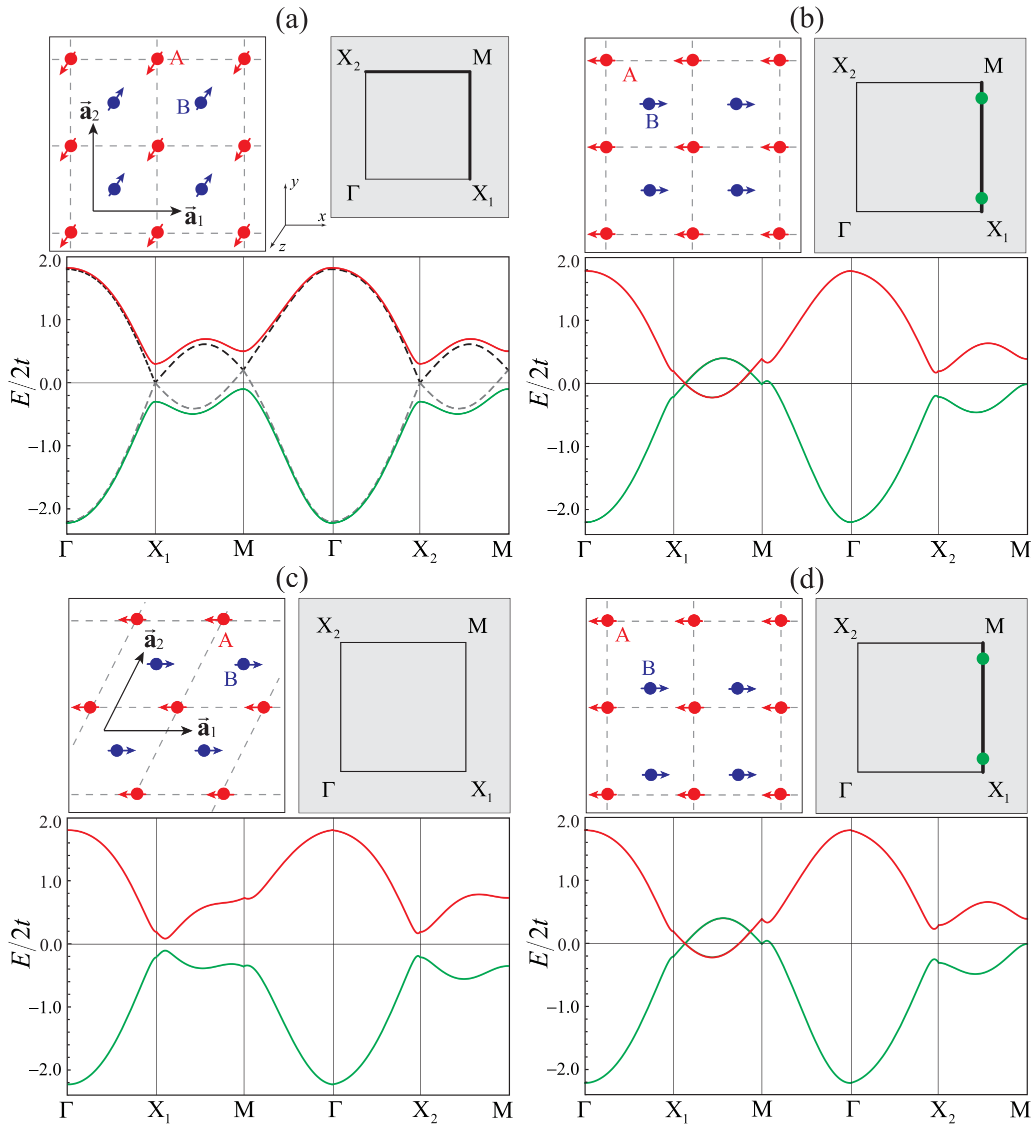

FIG. 2. Energy band with DPs protected by nonsymmorphic symmetries in an AFM lattice respecting $\mathcal{PT}$. The DPs are marked as green dots in the BZ. (a) DPs are gapped and cannot be protected by $\{C_{2\hat{x}}|\frac{1}{2}0\}$ and $\{C_{2\hat{y}}|0\frac{1}{2}\}$ when $\hat{\mathbf{n}} = \hat{z}$. (b) Two DPs located along the X_1-M line are protected by $\{M_{\hat{x}}|\frac{1}{2}0\}$ solely when $\hat{\mathbf{n}} = \hat{x}$. (c) Distortion in the $\langle 11 \rangle$ direction eliminates $\{M_{\hat{x}}|\frac{1}{2}0\}$ but keeps $\{M_{\hat{z}}|\frac{1}{2}\frac{1}{2}\}$, gapping the DPs. (d) Alternatively, B sites shifted in the y direction breaks $\{M_{\hat{z}}|\frac{1}{2}\frac{1}{2}\}$, but DPs still remain protected.

B. Symmetry breaking

Lowering the symmetry by external perturbations provides a toolbox to explore a wealth of topological phases. We start with the system as shown in Fig. 2(d). The $\{M_{\hat{x}}|\frac{1}{2}0\}$ breaking by distortion in Fig. 2(c) leads to a NI with gapped DPs. Displacing the B sites along [11] or $[1\bar{1}]$ always lead to NI phases. Quite different from $\mathcal{T}$-, $\mathcal{P}$-invariant 2D DSM where it lies at the boundary between QSH and NI [29], the 2D AFM DSM lies deeply in the NI phases. This is simply because the edge of a physical system always breaks $\mathcal{PT}$ and leads to gapped edge states, even though a nontrivial bulk Z_2 index may be defined. Similarly, the structure inversion asymmetry (SIA), by applying an electric field along the z axis, naturally breaks $\mathcal{PT}$ and adds a term $V\tau_3$, resulting in nondegenerate bands where DPs split into Weyl points, as shown in Fig. 3(a). Such Weyl points are located along the $k_x = \pi$ line and are not protected by symmetry. More interestingly, if both $\mathcal{PT}$ and $\{M_{\hat{x}}|\frac{1}{2}0\}$ are broken, a quantum anomalous Hall (QAH) state can be realized [38] and electrically controllable, as shown in Fig. 3(b). Furthermore, with the proximity effect to an s-wave superconductor, the realization of a chiral topological superconductor with external tunability is expected [39–42].

IV. DISCUSSION AND CONCLUSION

The AFM long-range order could exist in 2D. It would be interesting to study how the magnetic fluctuation and Coulomb interaction affect the stability of DPs, which is left to future work. In terms of realistic materials, the actual existence of such phases in known materials remains an open question. However, similar to TI materials, the 2D magnetic DSMs may exist in materials with both strong SOC and specific

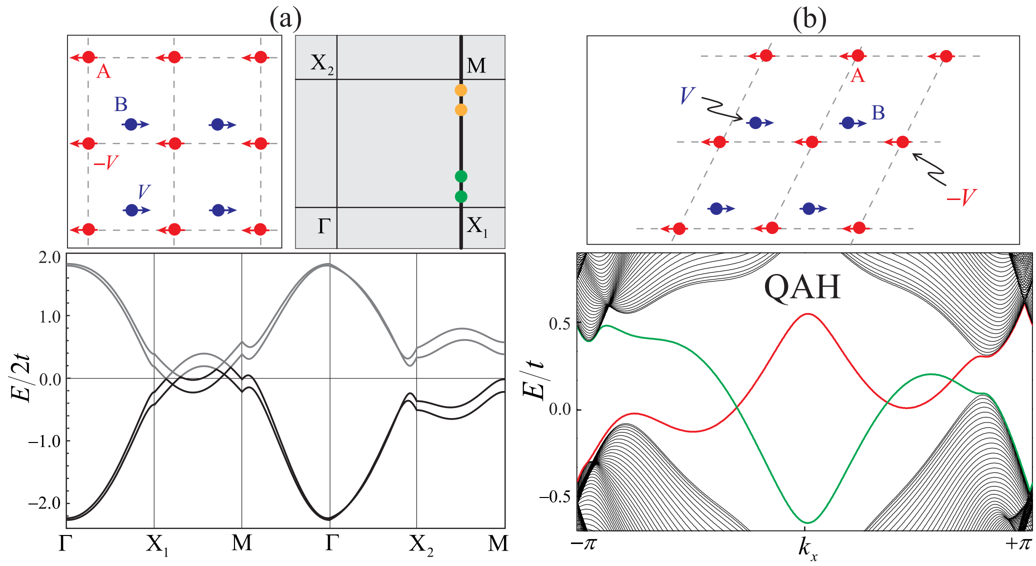

FIG. 3. Symmetry-breaking phases. (a) Breaking $\mathcal{PT}$ by SIA, while preserving $\{M_{\hat{x}}|\frac{1}{2}0\}$, leads to Weyl points (marked as yellow and green dots) on the $k_x = \pi$ line. (b) Breaking both $\mathcal{PT}$ and $\{M_{\hat{x}}|\frac{1}{2}0\}$ results in the QAH insulator. In the edge spectrum, the green and red lines are edge states located at upper and lower edges, respectively.

space-group symmetries. Furthermore, we comment on the possible candidate in the $A\text{MnBi}_2$ family of compounds (A = Ca, Sr, Eu, Yb) [43–48]. The transport experiments have already shown the 2D Dirac fermion behaviors in the bulk materials [47,48]. Take SrMnBi_2 for example; its bulk structure is in space group no. 139 ($I4/mmm$). For a monolayer of this material, the AFM order on Mn atoms is along the [001] direction, which breaks both $\mathcal{T}$ and $\mathcal{P}$ whereas $\mathcal{PT}$ still holds. The Bi atoms form two layers of square lattice, which is similar to the structure in Fig. 2(a), and determine most of the electronic structure [43–45]. The nonsymmorphic symmetries are $\{C_{2\hat{x}}|\frac{1}{2}\frac{1}{2}\}$ and $\{C_{2\hat{y}}|\frac{1}{2}\frac{1}{2}\}$. Therefore, the 2D DPs, if they exist in this material, can be protected by these symmetries, in principle. Unfortunately, this system shows *massive* Dirac fermions around the Fermi level, with a Dirac mass gap along the line Γ-M and M-X [43,44]. In fact, it is similar to the model in Eq. (4) with AFM ordering $\hat{\mathbf{n}}$ along the [001] direction.

In summary, we show that the 2D Dirac fermions could exist in AFM semimetals with $\mathcal{PT}$ symmetry, where the nonsymmorphic space-group symmetries play an essential role. The realistic AFM DSM materials remain unknown. However, considering the ongoing rapid progress in the field of 2D materials [49], together with the nonsymmorphic symmetries listed in Table I as a guidance, we are thus optimistic about the material search of the 2D AFM DSMs.

Note added. Recently, we became aware of an independent work on a similar problem [50]. However, their approach to 2D magnetic DSMs is different from our results.

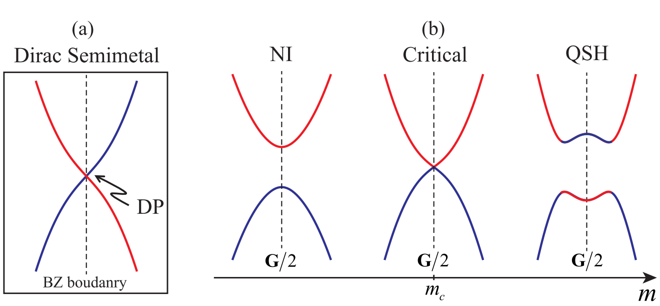

FIG. 4. (a) Nonsymmorphic symmetry-protected 2D DSMs with DPs located at the BZ boundary. (b) 2D DPs with accidental degeneracy appear at the phase transition between QSH and NI controlled by parameter m.

ACKNOWLEDGMENTS

The author is grateful to Haijun Zhang, Biao Lian, and Shoucheng Zhang for insightful discussions. This work is supported by the National Thousand-Young-Talents Program, the National Key Research Program of China under Grant No. 2016YFA0300703, the Natural Science Foundation of Shanghai under Grant No. 17ZR1442500, the Open Research Fund Program of the State Key Laboratory of Low-Dimensional Quantum Physics, through Contract No. KF201606, and by Fudan University Initiative Scientific Research Program.

APPENDIX A: $C_{n\hat{z}}$ AND $M_{\hat{z}}$ SYMMETRIES IN CASE A

The representations of the Γ matrices depend on the crystalline symmetry. If $\mathcal{P} = \pm\tau_0$, we get $\Gamma^{(1,2,3,4,5)} = (\tau_1, \sigma_3 \otimes \tau_2, \sigma_1 \otimes \tau_2, \sigma_2 \otimes \tau_2, \tau_3)$ and $d_a(\mathbf{k}) = d_a(-\mathbf{k})$ for $a = 1, \ldots, 5$. Similarly, if $\mathcal{P} = \pm\tau_3$, $\Gamma^{(1,2,3,4,5)} = (\sigma_3 \otimes \tau_1, \tau_2, \sigma_1 \otimes \tau_1, \sigma_2 \otimes \tau_1, \tau_3)$, and $d_a(\mathbf{k}) = -d_a(-\mathbf{k})$ for $a = 1, \ldots, 4$, $d_5(\mathbf{k}) = d_5(-\mathbf{k})$.

Here we give a short summary for the representations of $M_{\hat{z}}$ and $C_{n\hat{z}}$, and then give a detailed analysis for $C_{n\hat{z}}$ symmetry.

(i) $M_{\hat{z}}$ *symmetry*. $M_{\hat{z}}$ is the mirror symmetry with respect to the xy plane and requires $[M_{\hat{z}}, \mathcal{H}(\mathbf{k})] = 0$. It can be viewed as $M_{\hat{z}} = C_{2\hat{z}}\mathcal{P}$, where $C_{2\hat{z}}$ is the π rotation along the z axis. $M_{\hat{z}}$

follows the constraints $[\mathcal{T},M_{\hat{z}}]=0$, $M_{\hat{z}}^{\dagger}M_{\hat{z}}=1$, and $M_{\hat{z}}^2=e^{i\phi}$. The explicit form of $M_{\hat{z}}$ is (a) $M_{\hat{z}}=i\sigma_3\otimes\tau_1$, or $\sigma_3\otimes\tau_2$ when $|\mathcal{P}|=\tau_1$; (b) $M_{\hat{z}}=i\sigma_3$, or $i\sigma_3\otimes\tau_3$ when $|\mathcal{P}|=\tau_0,\tau_3$. The stable DPs can appear with $M_{\hat{z}}=\sigma_3\otimes\tau_2$ and $\mathcal{P}=\pm\tau_1$.

(ii) *$C_{n\hat{z}}$ symmetry.* $C_{n\hat{z}}$ is an n-fold rotation along the z axis, with $n=2,3,4,6$. The stable DPs can appear with $C_{\ell\hat{z}}$ ($\ell=2,4,6$) and $\mathcal{P}=\pm\tau_1$.

$C_{n\hat{z}}$ is the n-fold rotation along the z axis, with $n=2,3,4,6$. In order to obtain the explicit form of $C_{n\hat{z}}$, we can choose a basis where $C_{n\hat{z}}$ is diagonal as $C_{n\hat{z}}=\mathrm{diag}[u_A^{\uparrow},u_B^{\uparrow},u_A^{\downarrow},u_B^{\downarrow}]=\mathrm{diag}[\alpha_p,\alpha_q,\alpha_p^*,\alpha_q^*]$, where $\alpha_p=\exp[i\frac{2\pi}{n}(p+\frac{1}{2})]$ with $p=0,1,\ldots,n-1$. The invariance of the system under $C_{n\hat{z}}$ requires

$$C_{n\hat{z}}\mathcal{H}(k_+,k_-)C_{n\hat{z}}^{-1}=\mathcal{H}\big(k_+e^{i\frac{2\pi}{n}},k_-e^{-i\frac{2\pi}{n}}\big), \tag{A1}$$

where $k_\pm=k_x\pm ik_y$. Therefore, at the TRIM, the Hamiltonian commutes with $C_{n\hat{z}}$, i.e.,

$$[C_{n\hat{z}},\mathcal{H}(\mathbf{k}_{\mathrm{TRIM}})]=0. \tag{A2}$$

This is different from the $C_{2\hat{x}}$ and $M_{\hat{z}}$ cases, where invariant lines or plane exist in the BZ. We find that stable DPs can appear and are protected by $C_{2\hat{z}}$, $C_{4\hat{z}}$, $C_{6\hat{z}}$ together with $\mathcal{P}=\pm\tau_1$. The classification of 2D DSM protected by $C_{n\hat{z}}$ symmetry in case A is listed in Table I. From Table I, we can see that the $C_{4\hat{z}}$ case is consistent with the results obtained in Ref. [29]. The $C_{2\hat{z}}$ case is not independent from the $M_{\hat{z}}$ case in the main text, for in the presence of $\mathcal{P}$, $C_{2\hat{z}}=M_{\hat{z}}\mathcal{P}$.

Below we show the basic steps to see when the stable DPs can appear. As we discussed in the main text, the basic mechanism for the avoidable crossing of energy bands is to let the bands have different symmetry representations. The four Bloch states can be chosen as $|u_A^{\uparrow}\rangle$, $|u_B^{\uparrow}\rangle$, $|u_A^{\downarrow}\rangle$, and $|u_B^{\downarrow}\rangle$. Here, $|u_A^{\uparrow}\rangle$ and $|u_B^{\uparrow}\rangle$ have the $C_{n\hat{z}}$ eigenvalues $u_A^{\uparrow}$ and $u_B^{\uparrow}$, respectively. There are two distinct cases:

(i) When $\mathcal{P}=\pm\tau_0,\pm\tau_3$, the inversion operation will not flip the orbitals; thus the energy $E_{A,\uparrow}=E_{A,\downarrow}$, and $E_{B,\uparrow}=E_{B,\downarrow}$ at $\mathbf{k}_{\mathrm{TRIM}}$. Therefore, the four Bloch states are grouped into $(u_A^{\uparrow},u_A^{\downarrow})$ and $(u_B^{\uparrow},u_B^{\downarrow})$. In order to have a stable band crossing, one *necessary* condition is that these two groups must have different eigenvalues of $C_{n\hat{z}}$. Namely, $(u_A^{\uparrow},u_A^{\downarrow})$ are different from $(u_B^{\uparrow},u_B^{\downarrow})$. Due to $[C_{n\hat{z}},\mathcal{H}(\mathbf{k}_{\mathrm{TRIM}})]=0$, both $C_{n\hat{z}}$ and $\mathcal{H}(\mathbf{k}_{\mathrm{TRIM}})$ can be diagonal. The only possible form is $\mathcal{H}(\mathbf{k}_{\mathrm{TRIM}})=d_5\tau_3$. However, d_5 is even under $\mathcal{P}$, thus $d_5=m$, where m is the external parameters. In general, $m\neq 0$, and Eq. (A1) cannot constrain m to be zero; therefore, the stable Dirac points are not possible in this case.

(ii) Similarly, when $\mathcal{P}=\pm\tau_1$, inversion operation will switch the orbitals; therefore $E_{A,\uparrow}=E_{B,\downarrow}$, and $E_{B,\uparrow}=E_{A,\downarrow}$. Thus, $(u_A^{\uparrow},u_B^{\downarrow})$ must be different from $(u_B^{\uparrow},u_A^{\downarrow})$. This necessary condition rules out $C_{3\hat{z}}$. Moreover, we consider the only possible form of $\mathcal{H}$ at $\mathbf{k}_{\mathrm{TRIM}}$ is $\mathcal{H}(\mathbf{k}_{\mathrm{TRIM}})=d_1\sigma_3\otimes\tau_3$. However, $d_1(\mathbf{k})$ is an odd function, and thus d_1 vanishes. Furthermore, using Eq. (A1), one can get the possible forms of $d_a(\mathbf{k})$. Here we take $C_{4\hat{z}}$ for example; from the above symmetry analysis, the only possible form is $C_{4\hat{z}}=e^{\pm i\frac{\pi}{4}\sigma_3}\otimes\tau_3$. At the TRIM, all odd functions $d_{1,2,3,4}$ vanish, while $d_5(\mathbf{k}_{\mathrm{TRIM}})$ is an even function. But $C_{4\hat{z}}$ also force $d_5(\mathbf{k}_{\mathrm{TRIM}})$ to be odd. Therefore, d_5 vanishes at the TRIM and DPs can appear at such TRIMs. At the TRIM, the Hamiltonian is expanded as $d_{1,2,3,4,5}(\mathbf{k})=(0,0,vk_x,vk_y,0)$. More interestingly, $C_{6\hat{z}}$ symmetry could support the cubic Dirac fermions.

Here we point out that in case A with $\mathcal{P}$ symmetry, one can always construct the mirror symmetry $M_{\hat{n}_\perp}$ ($\hat{n}_\perp\perp\hat{z}$) from $C_{2\hat{n}_\perp}$ and $\mathcal{P}$ as $M_{\hat{n}_\perp}=C_{2\hat{n}_\perp}\mathcal{P}$. Here, $\hat{n}_\perp$ can be chosen to be $\hat{x}$ or $\hat{y}$. Therefore, $M_{\hat{n}_\perp}$ is not independent from $C_{2\hat{n}_\perp}$, and is not listed in Table I. However, in case B without $\mathcal{P}$, $M_{\hat{n}_\perp}$ is different from $C_{2\hat{n}_\perp}$, as we can see from Table I.

TABLE III. The nonsymmorphic symmetries which cannot protect the DPs in case B with $\mathcal{T}$ and $\mathcal{P}$ broken.

Symmetry	Half translation $\mathbf{t}$	DP protection
$\{C_{2\hat{x}}\|\mathbf{t}\}$	$\mathbf{t}=(\frac{1}{2},0)$	No
$\{C_{2\hat{y}}\|\mathbf{t}\}$	$\mathbf{t}=(0,\frac{1}{2})$	No
$\{M_{\hat{x}}\|\mathbf{t}\}$	$\mathbf{t}=(0,\frac{1}{2})$	No
$\{M_{\hat{y}}\|\mathbf{t}\}$	$\mathbf{t}=(\frac{1}{2},0)$	No
$\{M_{\hat{z}}\|\mathbf{t}\}$	$\mathbf{t}=(\frac{1}{2},0),(0,\frac{1}{2}),(\frac{1}{2},\frac{1}{2})$	No

APPENDIX B: NONSYMMORPHIC SYMMETRY WITH NO DP PROTECTION IN CASE B

Here we list in Table III the nonsymmorphic symmetries which cannot protect the DPs in case B.

APPENDIX C: ELECTRICALLY CONTROLLABLE QAH STATE

The parameters in Fig. 3(b) of the main text are $t_2=-0.1$, $\lambda_{\mathrm{so}}=0.5$, $\Delta=0.3$, $V=0.9$, and the four nearest-neighbor hoppings are $t_{AB}=(1.5,1.3,1.3,0.7)$. Meanwhile, the QAH state is electrically tunable, i.e., small V leads to the NI phase, as shown in Fig. 5.

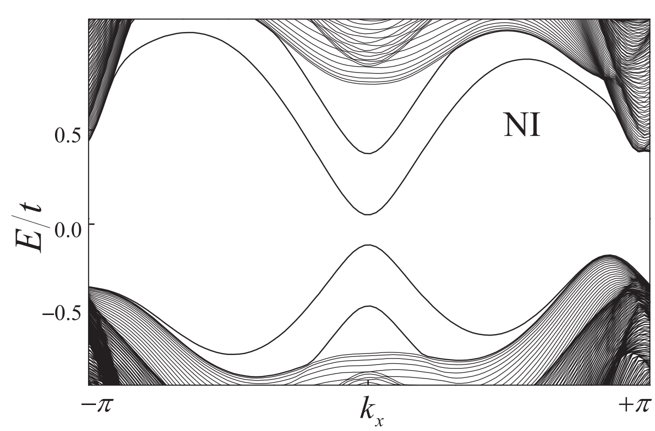

FIG. 5. The electrically tunable QAH state in both $\mathcal{PT}$ and $\{M_{\hat{x}}|\frac{1}{2}0\}$ broken AFM DSMs. The parameters $V=0.2$ and others are the same as in Fig. 3(b), which leads to a NI phase.

[1] M. Z. Hasan and C. L. Kane, Rev. Mod. Phys. **82**, 3045 (2010).
[2] X.-L. Qi and S.-C. Zhang, Rev. Mod. Phys. **83**, 1057 (2011).
[3] S. M. Young, S. Zaheer, J. C. Y. Teo, C. L. Kane, E. J. Mele, and A. M. Rappe, Phys. Rev. Lett. **108**, 140405 (2012).
[4] Z. Wang, Y. Sun, X.-Q. Chen, C. Franchini, G. Xu, H. Weng, X. Dai, and Z. Fang, Phys. Rev. B **85**, 195320 (2012).
[5] Z. Wang, H. Weng, Q. Wu, X. Dai, and Z. Fang, Phys. Rev. B **88**, 125427 (2013).
[6] J. A. Steinberg, S. M. Young, S. Zaheer, C. L. Kane, E. J. Mele, and A. M. Rappe, Phys. Rev. Lett. **112**, 036403 (2014).
[7] B.-J. Yang and N. Nagaosa, Nat. Commun. **5**, 4898 (2014).
[8] Z. K. Liu, B. Zhou, Y. Zhang, Z. J. Wang, H. M. Weng, D. Prabhakaran, S.-K. Mo, Z. X. Shen, Z. Fang, X. Dai, Z. Hussain, and Y. L. Chen, Science **343**, 864 (2014).
[9] Z. K. Liu, J. Jiang, B. Zhou, Z. J. Wang, Y. Zhang, H. M. Weng, D. Prabhakaran, S.-K. Mo, H. Peng, P. Dudin, T. Kim, M. Hoesch, Z. Fang, X. Dai, Z. X. Shen, D. L. Feng, Z. Hussain, and Y. L. Chen, Nat. Mater. **13**, 677 (2014).
[10] S. Borisenko, Q. Gibson, D. Evtushinsky, V. Zabolotnyy, B. Büchner, and R. J. Cava, Phys. Rev. Lett. **113**, 027603 (2014).
[11] J. Xiong, S. K. Kushwaha, T. Liang, J. W. Krizan, M. Hirschberger, W. Wang, R. J. Cava, and N. P. Ong, Science **350**, 413 (2015).
[12] B. J. Wieder, Y. Kim, A. M. Rappe, and C. L. Kane, Phys. Rev. Lett. **116**, 186402 (2016).
[13] B. Bradlyn, J. Cano, Z. Wang, M. G. Vergniory, C. Felser, R. J. Cava, and B. A. Bernevig, Science **353**, aaf5037 (2016).
[14] H. Watanabe, H. C. Po, M. P. Zaletel, and A. Vishwanath, Phys. Rev. Lett. **117**, 096404 (2016).
[15] A. H. Castro Neto, F. Guinea, N. M. R. Peres, K. S. Novoselov, and A. K. Geim, Rev. Mod. Phys. **81**, 109 (2009).
[16] S. Murakami, New J. Phys. **9**, 356 (2007).
[17] X. Wan, A. M. Turner, A. Vishwanath, and S. Y. Savrasov, Phys. Rev. B **83**, 205101 (2011).
[18] G. Xu, H. Weng, Z. Wang, X. Dai, and Z. Fang, Phys. Rev. Lett. **107**, 186806 (2011).
[19] A. A. Burkov and L. Balents, Phys. Rev. Lett. **107**, 127205 (2011).
[20] J. Liu and D. Vanderbilt, Phys. Rev. B **90**, 155316 (2014).
[21] S.-M. Huang, S.-Y. Xu, I. Belopolski, C.-C. Lee, G. Chang, B. Wang, N. Alidoust, G. Bian, M. Neupane, C. Zhang, S. Jia, A. Bansil, H. Lin, and M. Z. Hasan, Nat. Commun. **6**, 7373 (2015).
[22] H. Weng, C. Fang, Z. Fang, B. A. Bernevig, and X. Dai, Phys. Rev. X **5**, 011029 (2015).
[23] S.-Y. Xu, I. Belopolski, N. Alidoust, M. Neupane, G. Bian, C. Zhang, R. Sankar, G. Chang, Z. Yuan, C.-C. Lee, S.-M. Huang, H. Zheng, J. Ma, D. S. Sanchez, B. Wang, A. Bansil, F. Chou, P. P. Shibayev, H. Lin, S. Jia, and M. Z. Hasan, Science **349**, 613 (2015).
[24] B. Q. Lv, H. M. Weng, B. B. Fu, X. P. Wang, H. Miao, J. Ma, P. Richard, X. C. Huang, L. X. Zhao, G. F. Chen, Z. Fang, X. Dai, T. Qian, and H. Ding, Phys. Rev. X **5**, 031013 (2015).
[25] A. A. Soluyanov, D. Gresch, Z. Wang, Q. Wu, M. Troyer, X. Dai, and B. A. Bernevig, Nature (London) **527**, 495 (2015).
[26] Y. Sun, S.-C. Wu, M. N. Ali, C. Felser, and B. Yan, Phys. Rev. B **92**, 161107 (2015).
[27] J. Ruan, S.-K. Jian, H. Yao, H. Zhang, S.-C. Zhang, and D. Xing, Nat. Commun. **7**, 11136 (2016).
[28] P. Tang, Q. Zhou, G. Xu, and S.-C. Zhang, Nat. Phys. **12**, 1100 (2016).
[29] S. M. Young and C. L. Kane, Phys. Rev. Lett. **115**, 126803 (2015).
[30] B. J. Wieder and C. L. Kane, Phys. Rev. B **94**, 155108 (2016).
[31] Y. Chen and H.-Y. Kee, Phys. Rev. B **90**, 195145 (2014).
[32] J. W. F. Venderbos, Phys. Rev. B **93**, 115108 (2016).
[33] Y. X. Zhao and A. P. Schnyder, Phys. Rev. B **94**, 195109 (2016).
[34] B. Büttner, C. X. Liu, G. Tkachov, E. G. Novik, C. Brüne, H. Buhmann, E. M. Hankiewicz, P. Recher, B. Trauzettel, S. C. Zhang, and L. W. Molenkamp, Nat. Phys. **7**, 418 (2011).
[35] C. Fang, Y. Chen, H.-Y. Kee, and L. Fu, Phys. Rev. B **92**, 081201 (2015).
[36] C. J. Bradley and A. P. Cracknell, *The Mathematical Theory of Symmetry in Solids* (Clarendon, Oxford, 1972).
[37] C. L. Kane and E. J. Mele, Phys. Rev. Lett. **95**, 226801 (2005).
[38] X.-Y. Dong, S. Kanungo, B. Yan, and C.-X. Liu, Phys. Rev. B **94**, 245135 (2016).
[39] X.-L. Qi, T. L. Hughes, and S.-C. Zhang, Phys. Rev. B **82**, 184516 (2010).
[40] J. Wang, Q. Zhou, B. Lian, and S.-C. Zhang, Phys. Rev. B **92**, 064520 (2015).
[41] Q. L. He, L. Pan, A. L. Stern, E. Burks, X. Che, G. Yin, J. Wang, B. Lian, Q. Zhou, E. S. Choi, K. Murata, X. Kou, T. Nie, Q. Shao, Y. Fan, S.-C. Zhang, K. Liu, J. Xia, and K. L. Wang, arXiv:1606.05712.
[42] J. Wang, Phys. Rev. B **94**, 214502 (2016).
[43] J. Park, G. Lee, F. Wolff-Fabris, Y. Y. Koh, M. J. Eom, Y. K. Kim, M. A. Farhan, Y. J. Jo, C. Kim, J. H. Shim, and J. S. Kim, Phys. Rev. Lett. **107**, 126402 (2011).
[44] G. Lee, M. A. Farhan, J. S. Kim, and J. H. Shim, Phys. Rev. B **87**, 245104 (2013).
[45] Y. F. Guo, A. J. Princep, X. Zhang, P. Manuel, D. Khalyavin, I. I. Mazin, Y. G. Shi, and A. T. Boothroyd, Phys. Rev. B **90**, 075120 (2014).
[46] S. Borisenko, D. Evtushinsky, Q. Gibson, A. Yaresko, T. Kim, M. N. Ali, B. Büchner, M. Hoesch, and R. J. Cava, arXiv:1507.04847.
[47] A. Wang, I. Zaliznyak, W. Ren, L. Wu, D. Graf, V. O. Garlea, J. B. Warren, E. Bozin, Y. Zhu, and C. Petrovic, Phys. Rev. B **94**, 165161 (2016).
[48] H. Masuda, H. Sakai, M. Tokunaga, Y. Yamasaki, A. Miyake, J. Shiogai, S. Nakamura, S. Awaji, A. Tsukazaki, H. Nakao, Y. Murakami, T.-h. Arima, Y. Tokura, and S. Ishiwata, Sci. Adv. **2**, e1501117 (2016).
[49] K. S. Novoselov, A. Mishchenko, A. Carvalho, and A. H. Castro Neto, Science **353**, aac9439 (2016).
[50] S. M. Young and B. J. Wieder, arXiv:1609.06738.